

# Molecular Monolayer Nonvolatile Memory with Tunable Molecules\*\*

Junghyun Lee, Hojong Chang, Sangkwan Kim, Gyeong Sook Bang, and Hyoyoung Lee\*

With the development of the information industry, computer chips play a central role in information storage and have become highly integrated. Currently, there is increasing interest in the use of organic and polymer materials as nonvolatile memory elements.<sup>[1]</sup> Organic nonvolatile memory is a possible substitute for volatile dynamic random access memory (DRAM), which typically requires a data refresh every few milliseconds, and has the advantage of very low power consumption. However, limitations of the nanoscaled device fabrication of vapor-deposited organic resistive random access memory (ORRAM)<sup>[2]</sup> and spin-coated polymer resistive random access memory (PORAM)<sup>[3]</sup> have led to increased importance of molecular monolayer memory using organic self-assembled monolayers (SAMs). Several research groups have developed possible voltage-driven molecular memory devices possessing the advantages of fast response time and highly dense circuits over a photodriven circuit,<sup>[4]</sup> using a molecular monolayer for metal–molecule–metal (MMM) devices.<sup>[5]</sup> However, the use of molecular monolayers has been limited by low device yields, which are mainly attributed to electrical shorting,<sup>[6]</sup> especially for voltage-driven devices. As the top metal electrode is deposited onto the molecular monolayer, energetic metal atoms can degrade the SAM molecules,<sup>[7]</sup> and metal particles often penetrate the molecular monolayers to form metallic current paths.<sup>[8]</sup> To reduce the degree of electrical shorting, the following issues have been considered: the compactness and robustness of Langmuir–Blodgett (LB) films<sup>[9]</sup> and SAMs,<sup>[10]</sup> the use of bilayer SAMs;<sup>[11]</sup> a metal electrode with a nanosized surface area;<sup>[12]</sup> reduction of the surface roughness of the metal electrode;<sup>[13]</sup> a Pd nanowire<sup>[14]</sup> or single-walled carbon nanotube<sup>[15]</sup> as a substitute for the top metal electrode; and the use of a conducting polymer layer (PEDOT:PSS)<sup>[16]</sup> as a soft portion of the top metal electrode on the molecular monolayer. Although various prototype molecular monolayer

memory devices, including a photodriven example,<sup>[4]</sup> have been introduced, there are very few reports on molecular monolayer nonvolatile memory (MMNVM). For the fabrication of MMNVM, the design of redox-active molecular memory SAM materials becomes a critical factor, especially for the development of a voltage-driven MMNVM that requires direct contact measurement of the memory effect through a molecular monolayer between the bottom and top electrodes. It was recently demonstrated by scanning tunneling microscopy (STM) that Ru<sup>II</sup> terpyridine complexes without alkyl chains—metal-to-ligand charge-transfer (MLCT) complexes—have a voltage-driven molecular switch in the solid-state molecular junction.<sup>[17]</sup> In the fabrication of a molecular monolayer memory device, however, the direct use of Ru<sup>II</sup> terpyridine complexes without alkyl chains results in electrical shorting. In an implementation of molecular monolayer memory circuits with high yield, it is important to reduce the electrical shorting by modifying the Ru<sup>II</sup> terpyridine complexes with thiol-terminated alkyl chains of varying chain lengths on one or both sides.

Herein, we present the design, synthesis, and characterization of novel mono- and dialkylthiolate-tethered ruthenium(II) terpyridine hexafluorophosphate MLCT complexes and a novel fabrication of molecular monolayer devices. The hydrophilic terminal thiol group of the alkylthiolate-tethered Ru<sup>II</sup> terpyridine complexes was expected to interact with the hydrophilic sulfonic acid groups of PEDOT:PSS to prevent the penetration of soft and metal top electrodes into the SAMs and hence result in high yields.<sup>[16]</sup> It was also expected that as the number or length of the alkyl chains increases, the device yield of molecular monolayer memory would improve and its retention time would increase, thus guiding a new strategy for the development of volatile to nonvolatile memory. The direct measurement of the hysteretic *I*–*V* characteristics of the MMNVM, the write–multiple read–erase pulse cycles, and the retention time dependence on alkyl chain lengths are also reported.

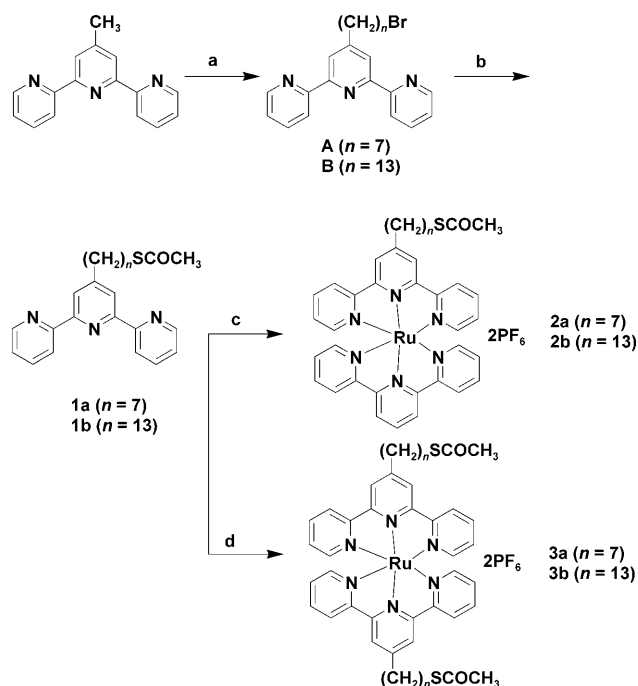
Novel mono- and dialkylthiolate-tethered ruthenium(II) terpyridine hexafluorophosphate [Ru<sup>II</sup>(tpy)(tpy(CH<sub>2</sub>)<sub>*n*</sub>Sac)](PF<sub>6</sub>)<sub>2</sub> (denoted [Ru<sup>II</sup>(tpy)(tpyC<sub>*n*</sub>S)]; tpy = terpyridine; *n* = 7, 13) and [Ru<sup>II</sup>{tpy(CH<sub>2</sub>)<sub>*n*</sub>Sac}<sub>2</sub>](PF<sub>6</sub>)<sub>2</sub> complexes (denoted [Ru<sup>II</sup>(tpyC<sub>*n*</sub>S)<sub>2</sub>], *n* = 7, 13), as shown in Scheme 1, were designed for the fabrication of a vertical MMM device using only a single monolayer. The synthesis and characterization of the new ruthenium complexes **2a,b** and **3a,b** that show a charging effect<sup>[17]</sup> are reported herein (see the Supporting Information for details).

The surfaces of the self-assembled molecular film (3.0 nm thickness) of [Ru<sup>II</sup>(tpyC<sub>*n*</sub>S)<sub>2</sub>] on Au were characterized using UV/Vis spectroscopy and spectroscopic ellipsometry. The very intense bands of the absorption spectrum of **3b** (Supporting Information, particularly Figure S1) could be

[\*] Dr. J. Lee, Dr. G. S. Bang, Prof. H. Lee  
NCRI, Center for Smart Molecular Memory  
Department of Chemistry, Sungkyunkwan University,  
Suwon 440-746 (Republic of Korea)  
Fax: (+82) 31-299-5934  
E-mail: hyoyoung@skku.edu  
H. Chang,<sup>[†]</sup> S. Kim  
Electronics and Telecommunications Research Institute (ETRI)  
138, Gajeongno, Yuseong-gu, Daejeon 305-700 (Republic of Korea)  
[†] Present address: Institute for Information Technology Convergence  
KAIST, Daejeon 305-701 (Republic of Korea)

[\*\*] This work was supported by the Creative Research Initiatives research fund (project title: Smart Molecular Memory) of the Ministry of Education Science and Technology (MEST) and the Korea Science and Engineering Foundation (KOSEF).

Supporting information for this article is available on the WWW under <http://dx.doi.org/10.1002/anie.200902990>.



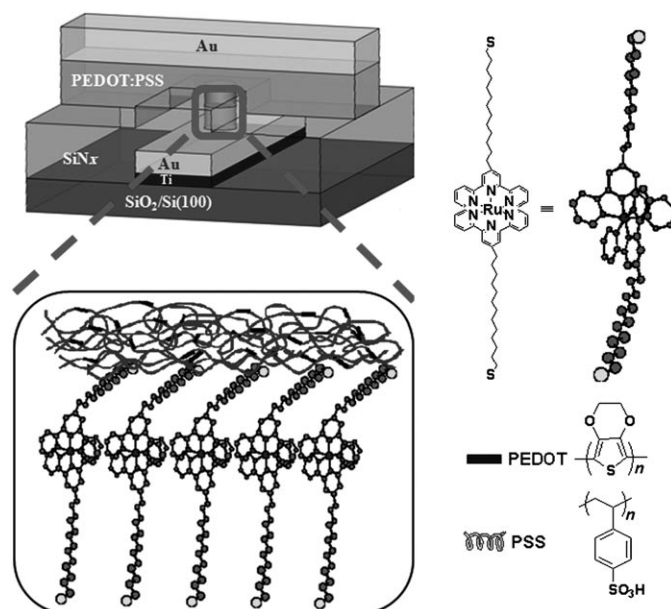
**Scheme 1.** Reagents and conditions: a) tetramethylpiperidine,  $nBuLi$ , 1,6-dibromohexane (**1a**) or 1,12-dibromododecane (**1b**) in THF at  $-78 \rightarrow -10^\circ C$  for 20 h; b) potassium thioacetate in DMF at RT for 1 h; c) 1.0 equiv  $[RuCl_3(ppy)_3]$  in EtOH at  $60^\circ C$ ,  $NH_4PF_6$ ; d) 0.5 equiv  $[RuCl_3(H_2O)_3]$  in EtOH/ $H_2O$  ( $v/v=3:1$ ) at  $110^\circ C$ ,  $NH_4PF_6$ .

assigned to ligand center  $\pi \rightarrow \pi^*$  transitions. The relatively intense and broad absorption band in the visible region, which is responsible for the dark red color, is due to the spin-allowed  $d \rightarrow \pi^*$  MLCT transition.<sup>[18]</sup> UV/Vis absorption and ellipsometry spectra of **3b** in  $CH_3CN$  and on a SAM are displayed in Figure S1 (Supporting Information). The peak shape of the self-assembled film is broadened more than that in the bulk solution. Although the maximum absorption peak of the self-assembled film was red-shifted by approximately 5.0 nm relative to that of the bulk solution, the peaks matched very well. The ruthenium complexes are electrochemically active. Cyclic voltammetric studies revealed that all ruthenium complexes exhibited pseudoreversible electron-transfer behavior with a pair of  $Ru^{II}/Ru^{III}$  redox peaks at approximately 1.2 V (versus  $Ag/AgCl$ ). To further confirm these SAMs, samples were examined using X-ray photoelectron spectroscopy (XPS). Figure S2 (Supporting Information) shows the XPS spectra of the SAM of **3b** on a gold substrate. In the C(1s) region (Supporting Information, Figure S2B), the binding energy for C(1s) was 284.7 eV, which is consistent with the majority of the carbon atoms being  $sp^2$  hybridized. To investigate the interaction of **3b** with the gold substrate, it was essential to scrutinize the S(2p) region. The measured S(2p<sub>3/2</sub>) binding energy of 162.0 eV was in excellent agreement with other studies.<sup>[19]</sup> A sulfonate peak at  $-168$  eV was not observed, which suggests that the SAM of **3b** adsorbed on gold as a thiolate.

The processing of a molecular device with diameters of 25  $\mu m$  is shown in Figure S3 (Supporting Information). A well diameter of 25  $\mu m$  from 5, 15, 25, and 40  $\mu m$  was chosen, as it

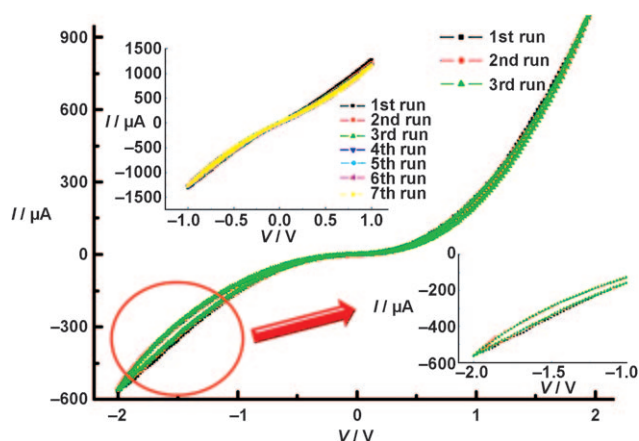
provided the highest device yield (see the Supporting Information for details).

Figure 1 depicts a schematic of the cross section of the device layout of PEDOT:PSS on the ruthenium complexes (PEDOT = poly(3,4-ethylenedioxythiophene), PSS = poly(4-styrenesulfonic acid)). The device yields of  $Ru^{II}$  complexes using **2a** and **2b** were in the range of 0–4 % (2 out of 48), whereas those of **3a** and **3b** were 19 % (14 out of 72) and 81 % (83 out of 103), respectively.



**Figure 1.** Schematic representation of the cross section of the device layout of a conducting polymer (PEDOT:PSS) on the ruthenium complex SAMs.

The devices were electronically stable and possessed thermal stability up to  $300^\circ C$ , indicating that decreasing the electrical shorting through modification of the  $Ru^{II}$  terpyridine complexes with thiolate-terminated alkyl chains was crucial in the improvement of device yield. In particular, one terminal thiol group of the dialkylthiols was introduced to attach the  $Ru^{II}$  complexes onto a gold surface. The other thiol group of the dialkylthiol allowed hydrophilic interactions with the sulfonic acid of PEDOT:PSS. This arrangement prevented permeation of PEDOT:PSS onto the SAMs, as the mono-alkylthiol could not contribute to hydrophilic interactions because of the hydrophobic terpyridine end group. In addition, longer alkyl chains effectively prevented penetration of the PEDOT:PSS and top metal electrode, resulting in a higher device yield. In fact, as the number of alkyl chains or the alkyl chain lengths increased, the device yield improved sharply from nearly 0 to 81 %. All current–voltage ( $I$ – $V$ ) measurements were performed in a vacuum to avoid the influence of moisture and oxygen, especially for PEDOT:PSS. Figure 2 shows the  $I$ – $V$  characteristics of the Au/**3b**/PEDOT:PSS/Au junction with a diameter of 25  $\mu m$ . The  $I$ – $V$  characteristics of the devices were recorded by scanning the applied voltage from 0 to +2 V and then to  $-2$  V, followed by a reverse scan from  $-2$  to +2 V. The positive bias



**Figure 2.** Hysteretic  $I$ - $V$  characteristics of the molecular monolayer device (Au/**3b**/PEDOT:PSS/Au). The  $I$ - $V$  characteristics of the device were recorded by scanning the applied voltage from 0 to +2 V and then to -2 V followed by a reverse scan from -2 to +2 V. Top inset: control experiment using PEDOT:PSS without ruthenium SAMs between the top and bottom electrodes. Bottom inset: magnification of the hysteretic  $I$ - $V$  curve.

corresponded to positive voltages applied to the top metal pad, whereas a negative bias corresponded to negative voltages applied to the top pad. The top inset of Figure 2 shows a control experiment using only PEDOT:PSS without ruthenium SAMs between the top and bottom electrodes. This experimental setup showed nearly ohmic behavior with kilohm resistance. The  $I$ - $V$  curve of Ru<sup>II</sup> complex **3b** was asymmetric (Figure 2). The negative bias region always indicated a larger current and hysteresis. An enlarged hysteretic  $I$ - $V$  curve is shown in the bottom inset of Figure 2. This result resembles the diagram reported for the [Ru<sup>II</sup>(bipyridyl)<sub>2</sub>(triazolopyridyl)] complex prepared by spin-coating with a thickness of 80 nm.<sup>[20]</sup>

Stable conductivity switching behavior makes it possible for nonvolatile molecular memory phenomena to be tested under a voltage pulse sequence, specifically, a write-read-erase-read (WRER) cycle. In such a cycle, the high (write) and low (erase) conducting states were repeatedly induced and the read states monitored in between the high and low conducting states. A section of the voltage sequence and corresponding current from the device is shown in Figure 3a,b.

The device can be programmed to a high conductivity state using a -1.5 V pulse and to a low conductivity state using a +1.5 V pulse with multiple current measurements for reading at -1.0 V. This device shows no significant degradation after several hundred write-and-erase cycles. This stable conductivity switching behavior made it possible for metal-SAM-conducting polymer-metal junctions to be used as nonvolatile memories with write-multiple read-erase-multiple read operations (Figure 3b). Each multiple reading was measured eight times after each write or erase pulse. The WRER cycles can be repeatedly performed in an excess of 300 cycles (Figure 3c).

Figure 4 shows the typical retention time measured under inert conditions. Once the device is switched to the ON state

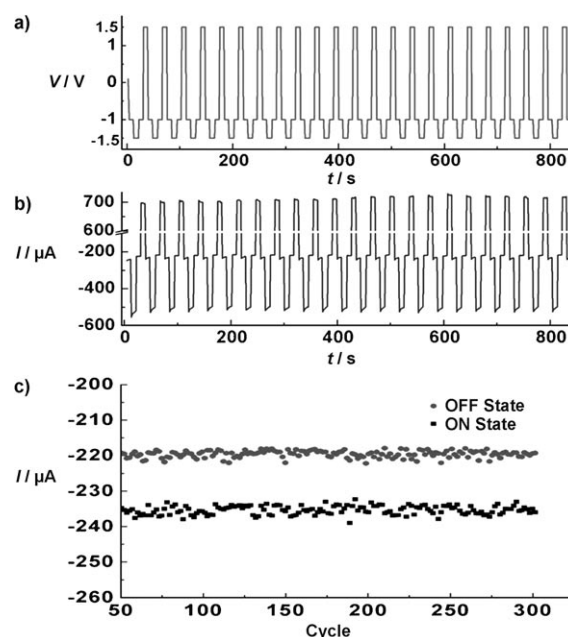


**Figure 3.** a,b) Write-multiple read-erase-multiple read (WRER) cycles of a molecular monolayer device containing Ru<sup>II</sup> complex **3b** for a rewritable data storage application. The writing, reading, erasing, and reading voltages were -1.5, -1, +1.5, and -1 V, respectively. c) Current in the ON state and OFF states as a function of the number of WRER cycles.  $3.0 \times 10^2$  cycles were tested in inert conditions.

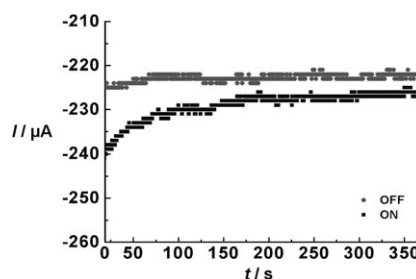


**Figure 4.** Retention times of the ON and OFF states of the molecular monolayer device, Au/**3b**/PEDOT:PSS/Au, probed with currents under -1.0 V. The ON and OFF states were induced by -2.0 V (writing) and 2.0 V (erasing), respectively.

by applying a negative voltage pulse at -2.0 V, this state was retained after 390 s with insignificant degradation. When the ON state was switched back to the OFF state by a positive voltage pulse applied at an amplitude of +2.0 V, this OFF state was sustained even after 390 s with little degradation. Conversely, in the case of shorter alkyl chains (**3a**), the retention time was reduced to near 200 s. For the application of MMNVM, the retention time of Ru complex **3b** remained sufficiently large compared with that of DRAM (a few milliseconds), and, furthermore, the retention time of **3b** could be extended to several days by utilizing a nanowire as a channel,<sup>[21]</sup> as shown in our previous report with **2a**.<sup>[22]</sup>

In addition, the ratio between the probe currents corresponded to the ON/OFF ratio obtained in the  $I$ - $V$  characteristics, as depicted in Figure 2. Although the ON/OFF ratio of

the molecular monolayer was not large compared with the 4–5 orders of magnitude of the ON/OFF ratio of our organic bulk memory device using the same materials with 60 nm thickness (Supporting Information, Figure S4), direct observation of the nonvolatile memory effect in the molecular monolayer was very meaningful for designing a nanoscaled circuit and architecture that did not require a large ON/OFF ratio under consideration of a faster response time and low power operation, and for fabricating large-array molecular memory devices toward the realization of ultimately miniaturized devices.

To understand the performance of the present MMNVM, the conduction mechanism for the switching behavior was investigated. It is known that the presence of large mobile counter anions ( $\text{PF}_6^-$ ) in the Ru complex and conducting polymer PEDOT:PSS, used as a soft portion of the top electrode, does not play an important role in the conduction mechanism.<sup>[17,20]</sup> Thus, the conductance switching mechanism of  $[\text{Ru}^{\text{II}}(\text{tpy}(\text{CH}_2)_n\text{S})_2]$  with alkyl chains ( $n = 7, 13$ ) should be similar to that of the  $[\text{Ru}^{\text{II}}(\text{tpy})(\text{tpyS})]$  complex without alkyl chains, previously reported by us.<sup>[17]</sup> The conductance switching mechanism was at least a two-step tunneling process whereby the electron first tunnels from the electrodes into the metal–ligand complex center (electron reduction), while maintaining an OFF state. The electron then tunnels out from the terpyridine ligand of the ruthenium complex to the electrodes (electron oxidation), while maintaining an ON state. The hysteresis observed was then the result of charging/uncharging of the self-assembled monolayer, which acts as a capacitor.<sup>[20]</sup> The transport mechanism, based on variable low-temperature measurements at only the ON or the OFF states, is direct tunneling, independent of temperature (see the Supporting Information for details).

In summary, a novel MMNVM was demonstrated using new  $\text{Ru}^{\text{II}}$  terpyridine complexes with thiol-terminated alkyl chains of different chain lengths on one or both sides. As predicted, the dialkyl chains and longer alkyl chains effectively prevented penetration of PEDOT:PSS and the top metal electrode into the SAMs, resulting in a higher device yield. With the dialkylthiol complex, the device yield increased to 81 %, even with a 25  $\mu\text{m}$  well. In addition, as the alkyl chain length was increased, the retention time increased. Write–multiple read–erase–multiple read pulse cycles were repeatedly operated at low driving voltages with a reasonable ON/OFF ratio. This device showed no significant degradation after several hundred pulse cycles. This is the first known development of a voltage-driven MMNVM that does not involve the use of state-of-the-art techniques and uses a commercially available micro-sized metal electrode well. Although the retention time and switching cycle remain far from satisfactory compared with current Si technology, our research on molecular monolayer memory can provide new insights into the design of voltage-driven functional molecules and the fabrication of MMNVM.

Received: June 3, 2009

Revised: August 4, 2009

Published online: September 30, 2009

**Keywords:** memory · molecular electronics · monolayers · ruthenium · self-assembly

- [1] J. C. Scott, L. D. Bozano, *Adv. Mater.* **2007**, *19*, 1452.
- [2] a) D. Tondelier, K. Lmimouni, D. Vuillaume, C. Fery, G. Haas, *Appl. Phys. Lett.* **2004**, *85*, 5763; b) W. Tang, H. Shi, G. Xu, B. S. Ong, Z. D. Popovic, J. Deng, J. Zhao, G. Rao, *Adv. Mater.* **2005**, *17*, 2307.
- [3] D. Ma, M. Aguiar, J. A. Freire, I. A. Hummelgen, *Adv. Mater.* **2000**, *12*, 1063.
- [4] A. J. Kronemeijer, H. B. Akkerman, T. Kudernac, B. J. V. Wees, B. L. Feringa, P. W. M. Blom, B. D. Boer, *Adv. Mater.* **2008**, *20*, 1467.
- [5] a) B. de Boer, M. M. Frank, Y. J. Chabal, W. Jiang, E. Garfunkel, Z. Bao, *Langmuir* **2004**, *20*, 1539; b) R. K. Smith, P. A. Lewis, P. S. Weiss, *Prog. Surf. Sci.* **2004**, *75*, 1; c) R. Haag, M. A. Rampi, R. E. Holmin, G. M. Whiteside, *J. Am. Chem. Soc.* **1999**, *121*, 7895.
- [6] a) M. D. Austin, S. Y. Chou, *Nano Lett.* **2003**, *3*, 1687; b) T. Kim, G. Wang, H. Lee, T. Lee, *Nanotechnology* **2007**, *18*, 315204.
- [7] G. L. Fisher, A. V. Walker, A. E. Hooper, T. B. Tighe, K. B. Bahnck, H. T. Skriba, M. D. Reinard, B. C. Haynie, R. L. Opila, N. Winograd, D. L. Allara, *J. Am. Chem. Soc.* **2002**, *124*, 5528.
- [8] J. Chen, M. A. Reed, A. M. Rawlett, J. M. Tour, *Science* **1999**, *286*, 1550.
- [9] a) Y. Chen, G. Y. Jung, D. A. A. Ohlberg, X. Li, D. R. Stewart, J. O. Jeppesen, K. A. Nielsen, J. F. Stoddart, R. S. Williams, *Nanotechnology* **2003**, *14*, 462; b) C. P. Collier, G. Mattersteig, E. W. Wong, Y. Luo, K. Beverly, J. Sampaio, F. M. Raymo, J. F. Stoddart, J. R. Heath, *Science* **2000**, *289*, 1172.
- [10] J. C. Love, L. A. Estroff, J. K. Kriebel, R. G. Nuzzo, G. M. Whitesides, *Chem. Rev.* **2005**, *105*, 1103.
- [11] G. S. Bang, H. Chang, J. R. Koo, T. Lee, R. C. Advincula, H. Lee, *Small* **2008**, *4*, 1399.
- [12] a) C. Zhou, M. R. Deshpande, M. A. Reed, L. Jones, J. M. Tour, *Appl. Phys. Lett.* **1997**, *71*, 611; b) W. Wang, T. Lee, M. A. Reed, *Phys. Rev. B* **2003**, *68*, 035416; c) M. A. Reed, J. Chen, A. M. Rawlett, D. W. Price, J. M. Tour, *Appl. Phys. Lett.* **2001**, *78*, 3735; d) N. Majumdar, N. Gergel, D. Routenberg, J. C. Bean, L. R. Harriott, B. Li, L. Pu, Y. Yao, J. M. Tour, *J. Vac. Sci. Technol. B* **2005**, *23*, 1417.
- [13] D. H. Kim, H. Lee, C. K. Song, C. Lee, *J. Nanosci. Nanotechnol.* **2006**, *6*, 3470.
- [14] C. Li, D. Zhang, X. Liu, S. Han, T. Tang, C. Zhou, W. Fan, J. Koehne, J. Han, M. Meyyappan, A. M. Rawlett, D. W. Price, J. M. Tour, *Appl. Phys. Lett.* **2003**, *82*, 645.
- [15] J. He, B. Chen, A. K. Flatt, J. J. Stephenson, C. D. Doyle, J. M. Tour, *Nat. Mater.* **2006**, *5*, 63.
- [16] H. B. Akkerman, P. W. M. Blom, D. M. D. Leeuw, B. D. Boer, *Nature* **2006**, *441*, 69.
- [17] K. Seo, A. V. Konchenko, J. Lee, G. S. Bang, H. Lee, *J. Am. Chem. Soc.* **2008**, *130*, 2553.
- [18] J. P. Sauvage, J. P. Collin, J. C. Chambron, S. Guillerez, C. Coudret, *Chem. Rev.* **1994**, *94*, 993.
- [19] Y. V. Zubavichus, Yu. L. Slovokhotov, M. K. Nazeeruddin, S. M. Zakeeruddin, M. Grätzel, V. Shklover, *Chem. Mater.* **2002**, *14*, 3556.
- [20] B. Pradhan, S. Das, *Chem. Mater.* **2008**, *20*, 1209.
- [21] M. Jung, J. S. Lee, W. Song, Y. Kim, S. D. Lee, N. Kim, J. Park, M. S. Choi, S. Katsumotos, H. Lee, J. Kim, *Nano Lett.* **2008**, *8*, 3189.
- [22] I. Choi, J. Lee, G. Jo, K. Seo, N. J. Choi, T. Lee, H. Lee, *Appl. Phys. Express* **2009**, *2*, 015001.